*Journal of Applied Electrochemistry* **30**: 323–331, 2000.
© 2000 *Kluwer Academic Publishers. Printed in the Netherlands.*


# Hydrogen fired PAFCs: an experimental investigation into the optimal utilization of impure, recycled hydrogen

J. SCHOLTA[1]*, B. ROHLAND[1] and H. WENDT[2]
[1]*Zentrum für Sonnenenergie- und Wasserstoff-Forschung, GB 3, Helmholtzstrasse 8, D 89081 Ulm, Germany;*
[2]*Institut für Chemische Technologie, TU Darmstadt, Petersenstrasse 35, D 64827 Darmstadt, Germany*
*(*author for correspondence, e-mail: jscholta@huba.zsw.uni-ulm.de*

Received 4 January 1999; accepted in revised form 18 August 1999

*Key words:* fuel cell, hydrogen recycle loop, operation parameters, PAFC operation

**Abstract**

Phosphoric acid fuel cells (PAFCs) had been developed for cogeneration plants based on natural gas as fuel. Operation of phosphoric acid fuel cells on hydrogen requires recycling of unspent hydrogen from the anode exhaust for obtaining highest efficiency. But recycling rates are limited due to accumulation of inert gases. Theoretical calculations and experimental data on optimizing this operation mode with respect to highest electrical energy efficiency are compared. The results are verified in a 100 $cm^2$ PAFC unit. From the data obtained with a Fuji 2 kW PAFC, the performance of large units with hydrogen recycling is predicted.

## 1. Introduction

Phosphoric acid fuel cells had been developed for cogeneration plants based on natural gas. Life time experiments extending to more than 38 000 h are reported [1, 2], and ONSI Corp. as the world's singular producer of commercial PAFCs claims that their PC 25 C units have a lifetime expectancy of 60 000 h. Although other cell types are able to cogenerate electric power and heat at even higher electrical efficiencies [3], availability and a relatively low price of PAFCs make this cell type today the most suitable for stationary applications. At present, only PAFC systems are commercially available. There are, however, still a number of problems being investigated.

Hydrogen from the chemical process industries and from gas grids which can be used for NG as well as for $H_2$-transport is a PAFC fuel which might gain importance in the future [4]. However, operating PAFCs on hydrogen instead of natural gas necessitates remarkable changes in fuel processing, hydrogen recycling and total process control. In principle, PAFCs fed with hydrogen can be operated in 'dead end' mode with purging at defined intervals, but for steady cell performance it would be advisable to recycle the hydrogen with a continuous purge which keeps the level of impurities and inerts at a constant level. In this work, PAFC performance under operation with recycled hydrogen is investigated experimentally and theoretically. The results are verified in a 100 $cm^2$ PAFC unit. Operational data obtained from a Fuji 2 kW PAFC were also obtained to allow for predicting more reliably the performance of larger PAFC units of 50 to 100 $kW_{el.}$ operated on recycled hydrogen. The intention is to find the optimal recycling conditions of impure hydrogen for large scale PAFC units.

## 2. Experimental details

### 2.1. *Labscale cell of 100 cm²*

The experimental 100 $cm^2$ cell used to measure all current/cell voltage correlations consisted of aluminium endplates with a thickness of 20 mm, copper plates for current collection, PTFE impregnated grooved graphite plates similar to those delivered by ETEK for membrane cells and appropriate PTFE-sealings. The cell was heated by means of two heaters which were inserted into the aluminium plates. The gases were introduced via the grooved graphite plates by internal manifolding. Commercial electrodes from E-Tech with a platinum loading between 0.35 and 0.45 mg $cm^{-2}$ for cathode and anode each were used.

The cell was operated in a test facility depicted in Figure 1. The anode was supplied with well defined mixtures of hydrogen, nitrogen and water vapour, the cathode was supplied with mixtures of oxygen, nitrogen and water vapour. The results presented in this work were obtained with oxygen at 20% gas utilization. Pipes carrying humidified gases from the humidifier to the cell were heated above 100 °C in order to prevent conden-

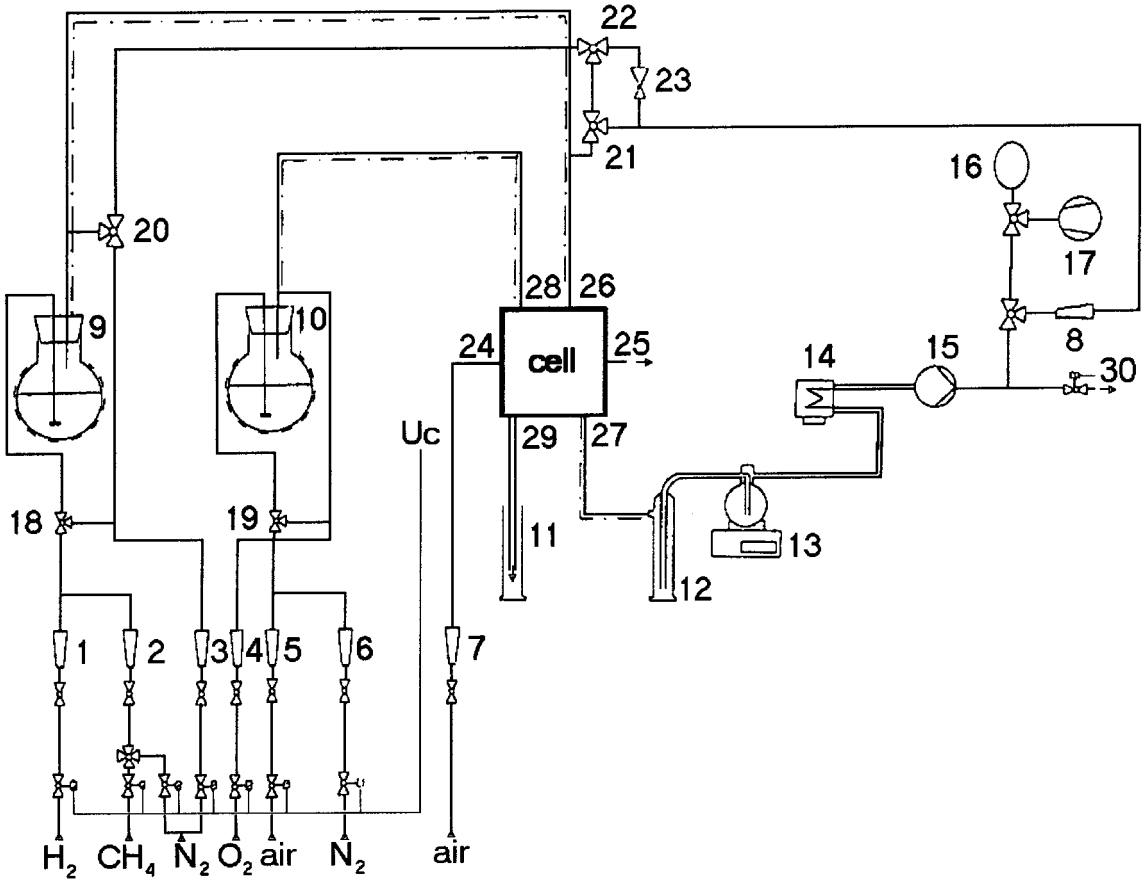


*Fig. 1.* Schematic flow sheet for measurements with the experimental 100 $cm^2$ cell operated on recycled hydrogen.

sation of water. A recycle loop allowed for operating the anode with recycled hydrogen. The water content of the anode off gas was determined gravimetrically by absorbing the water through concentrated phosphoric acid. The condensation unit (14) protected the circulation pump (15) from water and phosphoric acid. The circulation pump produced a pressure of up to 0.7 bar which was sufficient to operate the flow controller (8, Tylan General) in the recycle loop. The anode off gas was switched by valves (21) and (22) between recycle and nonrecycle operation mode. For recycle operation, the flow controller (1) was operated as flow meter and the flow rate was adjusted via the pressure regulating valve (23). Gas probes could be taken from the rubber balloon (16). The vacuum pump (17) was used for removal of rest gases. Valve (30) controls the anode outlet during recycle and non recycle operation. The cathode off gas left the cell via (11). If necessary, adjustable air cooling of the cell was provided by (7, 24, 25). Flasks (9) and (10) acted as humidifiers for the anode and cathode gas, and the water content was thermostated to 60 °C which complied with a water vapour content of 19.7 vol %.

Cell voltages were monitored automatically at intervals of one second. In case of voltage breakdown or mains failure purging with nitrogen and shorting the cell was performed automatically to avoid cell damage. The Jaissle potentiostat DAT90/10000 T-B which controlled current and power of the cell was operated in galvanostatic mode and was connected with the data acquisition and control-unit HP 3652A. All potentials were read from this unit which also controlled the gas flow rates. In case of improper operation, the cell was automatically shut down to a safe standby mode.

Relevant operational parameters were cell temperature, concentration of inerts (e.g., $CH_4$, $N_2$, $CO_2$) in the fuel and gas utilization. In this work, $N_2$ was used as inert gas. Its content in the feed hydrogen was varied between one and forty vol % (referred to pure $H_2$). Comparability of the inerts $CH_4$ and $N_2$ with respect to cell performance losses was verified in nonrecycle operation cell tests. In this operation mode, the dew point of inlet hydrogen was kept at 60 °C. In recycle operation mode, no external humidification was used. The cell temperature was kept constant at 180 °C. From those data, a model for optimised cell operation on inert gas containing hydrogen with recycling of the anode gas was developed and optimal performance predicted from this model was demonstrated in a small scale unit [5].

### 2.2. *Fuji-2 kW-PAFC*

The Fuji 2 kW-PAFC consisted of 30 cells each with 650 $cm^2$ electrode area. During standstill the cell was electrically heated and kept at 50 °C in order to prevent solidification of the electrolyte. Cell control and data monitoring of the 2 kW unit was comparable to that of

the lab cell. By flow controllers and a vaporiser the supply of pure, humidified and inert gas containing hydrogen was established. Temperature and pressure sensors were positioned in all relevant gas and cooling loops. The cooling loop consisted of a heat exchanger operating with a cooling oil on the primary and cold water on the secondary side and a pumping unit. The circulation speed in the primary loop was $9\,\mathrm{l\,min^{-1}}$. During operation, temperature regulation was provided by a switching valve in the secondary cooling loop. In case of malfunction an automatic shut down procedure ran the cell down to a standby mode. The d.c.-current was converted to AC 220 V, 50 Hz and fed to the grid.

## 3. Results

The Fuji fuel cell of 2 kW rated electric power was operated over a total of more than 2000 h. More than 20 user defined startup and shutdown procedures were performed without detectable cell degradation. Current–voltage correlations of the stack were measured to determine the dependence of the cell voltage on gas utilization and inert gas content. Performance data of the 2 kW PAFC are given in [6].

### 3.1. *Energy, mass balances and energy efficiency for hydrogen recycling*

Using the mass balances and the relationship between inert gas fraction ($x_\mathrm{i}$), single pass utilization ($X_\mathrm{anode}$) on one hand and cell voltage on the other, the electrical energy efficiency can be calculated and optimized.

The energy balances of a fuel cell equates the reaction enthalpy with the produced electricity and heat:

$$-\Delta H(\dot{N}_{\mathrm{H_2,inlet}} - \dot{N}_{\mathrm{H_2,outlet}}) = U_\mathrm{Stack} I + \dot{Q} \tag{1}$$

with $\Delta H$ equaling the molar heat of combustion of hydrogen. The heat produced was related to the enthalpy of hydrogen oxidation:

$$\dot{Q} = \left(-\frac{\Delta H}{2F} - U_\mathrm{single\ cell}\right) I\, n \tag{2}$$

where $n$ is the number of cells. The electrical cell efficiency was given by the ratio of the cell voltage and the voltage equivalent to the reaction enthalpy $\Delta H$:

$$\eta_\mathrm{cell} = \frac{U_\mathrm{single\ cell}}{-\Delta H/2F} = \frac{(U\,I)_\mathrm{Stack}}{-\dot{N}_\mathrm{fuel,in}\ \Delta H_\mathrm{combustion}} \tag{3}$$

We define

$$X_\mathrm{util} = \frac{\dot{N}_{\mathrm{H_2,conv}}}{\dot{N}_{\mathrm{H_2,in}}} \tag{4}$$

If hydrogen is recycled, the d.c. efficiency is

$$\eta_\mathrm{d.c.} = \eta_\mathrm{cell} X_\mathrm{anode} \tag{5}$$

Our major interest is in these both factors. If a coefficient $\alpha$, the 'purge rate', is defined:

$$\alpha \equiv \frac{\dot{N}_{\mathrm{H_2,purge}}}{\dot{N}_{\mathrm{H_2,conv}}} \tag{6}$$

the d.c. efficiency is the product of the inert gas fraction and anode utilization-dependent cell efficiency and a purge ratio-dependent factor:

$$\eta_\mathrm{d.c.} = \eta_\mathrm{cell}(x_\mathrm{i}, x_\mathrm{anode})\left(\frac{1}{1+\alpha}\right) \tag{7}$$

The steady state inlet inert gas fraction $x_\mathrm{i}$ of recycled hydrogen depends on the inert gas concentration $x_{\mathrm{i}0}$ of the hydrogen feed, the single pass anode utilization $X$ and the purge rate $\alpha$.

$$x_\mathrm{i} \approx \frac{x_{\mathrm{i}0}(1 - X_\mathrm{anode})}{x_{\mathrm{i}0}(1 - X_\mathrm{anode}) + \alpha} \tag{8}$$

where $x_{\mathrm{i}0}$ is the initial inert gas concentration of inlet hydrogen. This equation is derived from the mass balance for the inert components under steady state conditions, establishing the equality of the inlet flow and the outlet flow rate of inerts:

$$\dot{N}_{\mathrm{H_2,conv}} \frac{x_{\mathrm{i}0}}{1 - x_{\mathrm{i}0}} (1 + \alpha) \equiv \dot{N}_{\mathrm{H_2,conv}} \frac{x'_\mathrm{i}}{1 - x'_\mathrm{i}} \alpha \tag{9}$$

$x'_\mathrm{i}$ represents the inert gas concentration at the fuel cell outlet which is higher than the inert mol fraction of the recycled hydrogen at the cell inlet. In a real system only the bleedstream coefficient $\alpha'$ with

$$\alpha' \equiv \frac{\dot{N}_\mathrm{out}}{\dot{N}_{\mathrm{H_2,conv}}} \tag{10}$$

can be adjusted. $\alpha'$ equals:

$$\alpha' = \frac{\alpha}{1 - x'_\mathrm{i}} \tag{11}$$

Increasing the purge ratio $\alpha$ diminishes the inert mol fraction $x_\mathrm{i}$ in the recycled gas and results in increased cell efficiency. On the other hand, the utilization $\eta_\mathrm{util}$ decreases because of increasing hydrogen losses. Being the product of both factors, $\eta_\mathrm{d.c.}$ shows a maximum at adequate $\alpha$ values, that is, $\eta_\mathrm{d.c.}$ can be optimized if the dependency of $\eta_\mathrm{cell}$ on $x_\mathrm{i}$ and anode gas utilization $X_\mathrm{anode}$ is known.

### 3.2. *Current–voltage curves, modelling and operation with recycled hydrogen of a labscale PAFC*

Measuring the single cell voltages at 150 °C for different entrance conditions, $x_\mathrm{i}$, and different utilizations, $X$, which together with the molar flow rate of feed hydrogen define the total current, allow to mathemat-

ically model the $U, x_i, X$ relation. The measured data are collected in Table 1. The empirical polynomial equation (Equation 12) reflects the measured cell voltages as a function of $x_i$ and $X$ for a current density of 100 mA cm$^{-2}$.

A comparison of measured data and data from the polynomial equation (12) show an agreement within less than 2 mV and a mean deviation of less than ±0.3 mV. The polynomial equation is expressed as follows:

$$U = a + bX_{\text{anode}} + cX_{\text{anode}}^2 + dX_{\text{anode}}^3 + eX_{\text{anode}}^4 + \left(f + gX_{\text{anode}} + hX_{\text{anode}}^2 + iX_{\text{anode}}^3 + jX_{\text{anode}}^4\right)x_i + \left(k + lX_{\text{anode}} + mX_{\text{anode}}^2 + nX_{\text{anode}}^3 + oX_{\text{anode}}^4\right)x_i^2 \quad (12)$$

The fifteen coefficients $a$ to $o$ are: $a = 605.5 \pm 3.0$, $b = 3.8 \pm 0.1$, $c = -0.168 \pm 0.002$, $d = 0.002\,92 \pm 0.000\,03$, $e = -(179 \pm 6) \times 10^{-7}$, $f = 382 \pm 17$, $g = -44.4 \pm 0.3$, $h = 1.739 \pm 0.006$, $i = -0.028\,23 \pm 0.000\,09$, $j = (167 \pm 1) \times 10^{-6}$, $k = -1121 \pm 33$, $l = 130.3 \pm 0.7$, $m = -5.27 \pm 0.01$, $n = 0.0883 \pm 0.0002$ and $o = -(5625 \pm 29) \times 10^{-7}$.

In a second step the laboratory cell was operated more than 500 h in recycle operation mode and the measured cell voltages were compared with the predicted values using Equations 7, 8 and 12. The results are collected in Table 2.

*Table 1.* Measured and calculated cell voltage of lab scale PAFC (active area of 100 cm$^2$) at 100 mA cm$^{-2}$ dependent on inlet inert gas concentration and anode gas utilization at 150 °C, data for dry gases

| $x_i$ | $x_i'$ | Anode gas utilization/% | Measured cell voltage/mV | Cell voltage/mV (Equation 12) |
|---|---|---|---|---|
| 0 | 0.00 | 20 | 635.3 | 635.2 |
| 0.1 | 0.12 | 20 | 633.8 | 634.1 |
| 0.2 | 0.24 | 20 | 632.7 | 632.8 |
| 0.3 | 0.35 | 20 | 631.7 | 631.4 |
| 0.4 | 0.45 | 20 | 629.7 | 629.8 |
| 0 | 0.00 | 30 | 633.3 | 633.3 |
| 0.1 | 0.14 | 30 | 631.7 | 631.7 |
| 0.2 | 0.26 | 30 | 629.7 | 629.5 |
| 0.3 | 0.38 | 30 | 626.9 | 626.8 |
| 0.4 | 0.49 | 30 | 623.4 | 623.4 |
| 0 | 0.00 | 40 | 631.0 | 630.7 |
| 0.1 | 0.16 | 40 | 629.4 | 630.1 |
| 0.2 | 0.29 | 40 | 626.4 | 626.7 |
| 0.3 | 0.42 | 40 | 621.0 | 620.8 |
| 0.4 | 0.53 | 40 | 612.0 | 612.2 |
| 0 | 0.00 | 50 | 630.5 | 630.0 |
| 0.1 | 0.18 | 50 | 628.3 | 629.4 |
| 0.2 | 0.33 | 50 | 624.2 | 623.5 |
| 0.3 | 0.46 | 50 | 613.3 | 612.3 |
| 0.4 | 0.57 | 50 | 595.4 | 595.9 |
| 0 | 0.00 | 60 | 629.4 | 629.2 |
| 0.1 | 0.22 | 60 | 627.5 | 628.0 |
| 0.2 | 0.38 | 60 | 616.8 | 616.8 |
| 0.3 | 0.52 | 60 | 595.8 | 595.7 |
| 0.4 | 0.63 | 60 | 564.5 | 564.6 |
| 0 | 0.00 | 70 | 623.7 | 622.3 |
| 0.1 | 0.27 | 70 | 620.5 | 622.8 |
| 0.2 | 0.45 | 70 | 601.0 | 602.4 |
| 0.3 | 0.59 | 70 | 565.1 | 560.9 |
| 0.4 | 0.69 | 70 | 496.5 | 498.4 |

The experimental results of the 500 h test performed with the laboratory scale 100 cm$^2$ PAFC with hydrogen recycling verified the expected inert gas concentration and the predicted d.c. efficiency. Figure 2 shows the time chart for $\alpha' = 0.006$ and 0.012. The repeated voltage gain is caused by interval purging (2 and 4 h). The measured data of Table 2 are in good agreement if a gas leakage rate of 0.085 ml min$^{-1}$ is accomplished for. This leakage rate is included in the $\alpha'$-values and is of reasonable order of magnitude compared to a recirculation rate of 100 ml min$^{-1}$.

### 3.3. *Modelling current–voltage curves of the 2 kW PAFC stack*

The voltage of singular cells of the stack is obtained by substracting of the anode and cathode overpotential and the ohmic potential drop in the cell from the standard equilibrium cell voltage $U^\circ$.

$$U_{\text{cell}} = U^\circ - \eta_{\text{anode}} + \eta_{\text{cathode}} - U_{\text{IR}} \quad (13)$$

with

$$U^\circ = -\frac{\Delta G^\circ}{2F} \quad (14)$$

The temperature dependence of $U^\circ$ is determined by the reaction entropy:

$$\frac{dU^\circ}{dT} = -\frac{\Delta S^\circ}{2F} \quad (15)$$

The anode overpotential is essentially due to concentration polarization and reads, according to an equation derived by Stonehart et al. [7].

$$\eta_{\text{anode}} = \frac{RT}{2F}\left(\frac{i}{A_i\sqrt{20FW_{\text{Pt}}S_{\text{Pt}}D_{\text{H}_2}C(\text{H}_2)i_0/L}} - \ln(\bar{x}_{\text{H}_2})\right) \quad (16)$$

In this equation $A_i$ is a dimensionless number ≈1, $W_{\text{Pt}}$ the platinum loading in mg cm$^{-2}$, $S_{\text{Pt}}$ the surface area of Pt/gram, $D_{\text{H}_2}$ the diffusion coefficient of hydrogen in

*Table 2.* Measured and calculated cell voltages of the laboratory scale PAFC in recycle operation mode, $i$ = 100 mA cm$^{-2}$, recycle loop flow rate = 0.2 l min$^{-1}$, 33% single pass utilization

| $\alpha'$ | Cell voltage /mV | Gas leak rate /cm$^3$ min$^{-1}$ | $x_{i0}$ | $\alpha_{\text{calc.}}$ | $x_{i,\text{calc.}}$ | Cell voltage (Equation 12 /mV) |
|---|---|---|---|---|---|---|
| 0.095 | 675 | 0.085 | 0.0012 | 0.0936 | 0.01 | 679 |
| 0.048 | 678 | 0.085 | 0.0012 | 0.0459 | 0.03 | 679 |
| 0.024 | 680 | 0.085 | 0.0012 | 0.0220 | 0.05 | 679 |
| 0.012 | 678 | 0.085 | 0.0012 | 0.0101 | 0.11 | 678 |
| 0.006 | 675 | 0.085 | 0.0012 | 0.0041 | 0.23 | 675 |
| 0.003 | 660 | 0.085 | 0.0012 | 0.0011 | 0.52 | 660 |

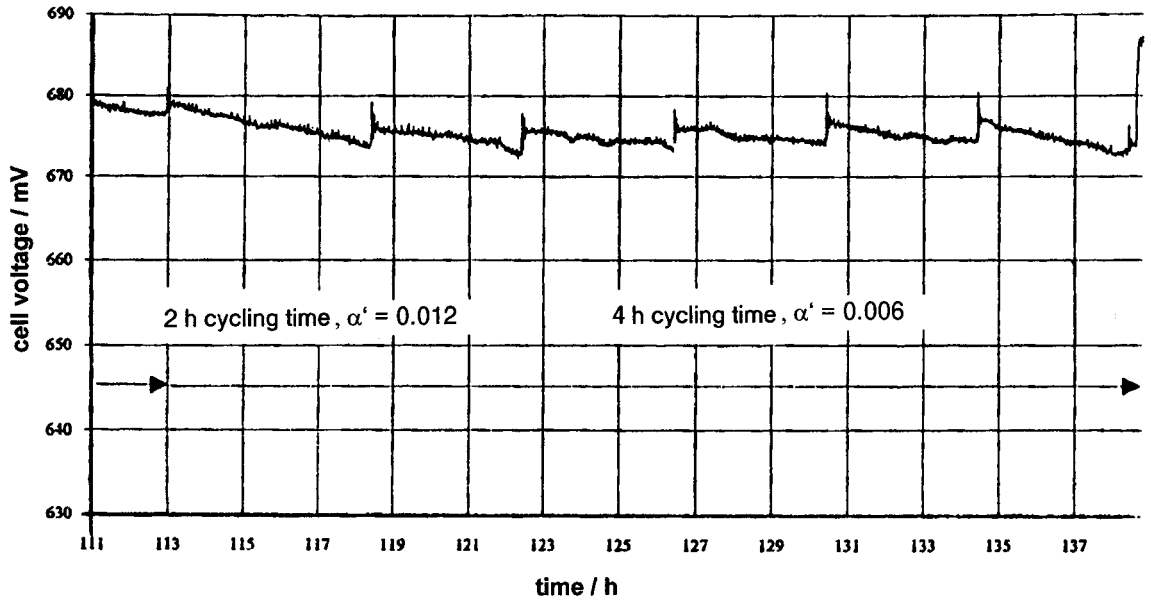


*Fig. 2.* Time chart of 100 $cm^2$ PAFC in recycle operation mode, $\alpha' = 0.012$ (2 h) and 0.006 (4 h), $i = 100$ mA $cm^{-2}$, recycle loop flow rate 0.2 l $min^{-1}$, 33% single pass utilization.

phosphoric acid, $C(H_2)$ the solubility of hydrogen according to Henry's law, $L$ the electrode thickness.

In Equation 16 the term

$$\bar{x}_{H_2} = 1 - \bar{x}_i = 1 - \frac{x_i}{2}\left[1 + \frac{1}{1 - (1 - x_i)X_{anode}}\right] \qquad (17)$$

has to be inserted. The cathode overpotential is essentially charge transfer controlled and reads:

$$\eta_{cathode} = b \lg\left(\frac{i}{i_0^*(\bar{x}_{O_2})^{1/2}}\right) - \frac{RT}{4F} \ln(\bar{x}_{O_2}) \qquad (18)$$

Here for $\bar{x}_{O_2}$ Equation 19 should be inserted:

$$\bar{x}_{O_2} = 1 - \frac{1}{2}(1 - x_{O_2})\left(1 + \frac{1}{1 - x_{O_2}X_{cathode}}\right) \qquad (19)$$

In this equation $b$ is the Tafel-slope ($\sim$90 mV $dec.^{-1}$) and $i_0^*$ the cathode exchange current density ($\sim 5\,\mu$A $cm^{-2}$ electrode area).

The ohmic losses are described by

$$U_{IR} = R' i \qquad (20)$$

with a temperature-dependent specific cell resistance $R'$.

In numerical terms the following is obtained:

$$U^\circ = 1.1588 - 0.000\,250\,7\ (T_{cell}/^\circ C - 126.85)\,V \qquad (21)$$

$$\eta_{anode} = \frac{T/^\circ C + 273.15}{23208} \times \left[\frac{0.2403\, i/mA\,cm^{-2}}{(T/^\circ C)^{7/8}[0.01371(T/^\circ C) - 1]^{1/2}\bar{x}_{H_2}{}^{1/2}} - \ln(\bar{x}_{H_2})\right] V \qquad (22)$$

$$\eta_{cathode} = -0.089 \lg i/mA\,cm^{-2} + (0.0487 + 4.95 \times 10^{-5}\, T/^\circ C)\lg(\bar{x}_{O_2}) - \left(\frac{167.5}{T/K} - 0.196\right) V \qquad (23)$$

$$U_{IR} = i/mA\,cm^{-2}\left(-0.33 + \frac{347.1}{T/K}\right) V \qquad (24)$$

The comparison of stack performance and single cell and stack data obtained from Equations 21–24 is shown in Figure 3. The deviation of modelled data and experimental values in a temperature range from 130 to 160 °C and a load range from 25 and 100% of full load is less than 3%, usually 1% or less.

### 3.4. *Optimizing electrical cell efficiency*

Based on the model described by Equations 21–24 calculated cell efficiencies against current density at temperatures ranging from 100 to 200 °C are shown in Figures 4 and 5. Figure 4 shows the data for pure hydrogen whereas Figure 5 shows the cell efficiencies for reformer gas with 35% inert gas concentration. With pure $H_2$ at current densities of 200 mA $cm^{-2}$ which equals to nominal load, the cell efficiency ranges from 41% at an operating temperature of 100 °C to 52% at 200 °C. With 35% inerts 38% at 100 °C and 51% at 200 °C efficiencies are achieved. At higher temperatures, the efficiency gain in pure $H_2$ becomes relatively lower. Because of corrosion effects [6] at the carbon support of the cathode catalyst at very high temperatures a moderate temperature regime (160–180 °C) seems to be preferable although it is known that the PAFC unit PC 25C of ONSI Inc. is operated at 200 °C. At 180 °C

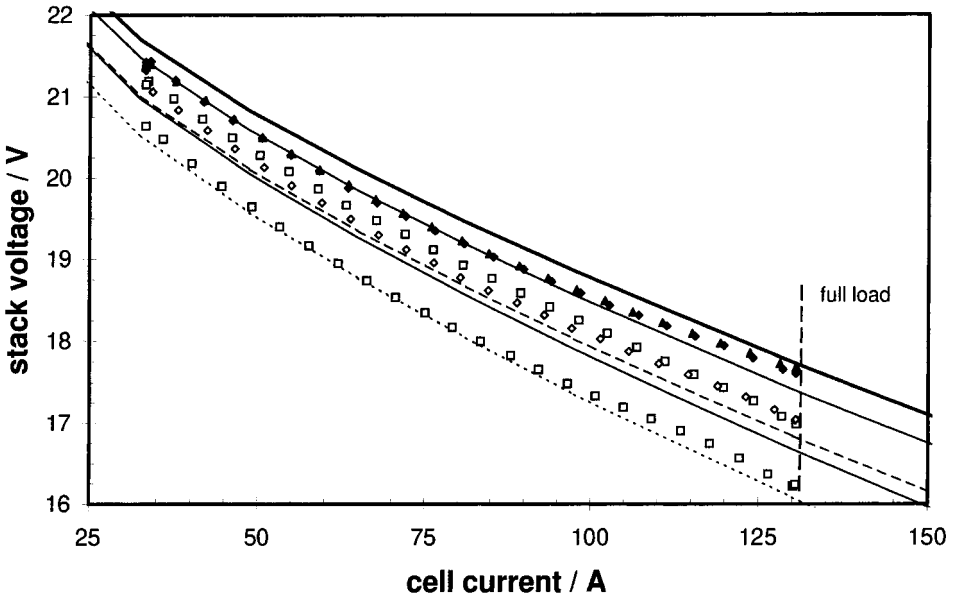


*Fig. 3.* Comparing calculated and experimental current–voltage characteristics measured with the Fuji 2 kW-PAFC-stack (80% anode gas utilization, 50% cathode gas utilization). Lines: model; signs: experimental values. Key: (- -□- -) 130 °C, 35% $CO_2$; (—□—) 130 °C, 0% $CO_2$; (–◇–) 150 °C, 35% $CO_2$; (—◆—) 150 °C, 0% $CO_2$; and (—▲—) 160 °C, 0% $CO_2$.

and nominal power, that is, 200 mA $cm^{-2}$ cell efficiencies of 49% for pure hydrogen and 47.6% for reformer gas, respectively, are obtained.

### 3.5. *Influence of hydrogen recycling on the electrical efficiency*

Applying to the model of the 2 kW PAFC (Equations 21–24) the mass balance-based Equation 8 in Equation 7 the resulting d.c. efficiency can be optimised with respect to relevant operation parameters. All data used and calculated in this section are valid for 160 °C cell temperature.

#### 3.5.1. *Effect of single pass utilization*

According to Equation 7 d.c. efficiencies depend not only on the inert inlet concentration $x_{i0}$ and the bleedstream $\alpha'$ but also on the single pass utilization $X_{single}$ of the anode gas. This is shown in Figure 6 which depicts the dependence of $\eta_{d.c.}$ at optimized purge rates on $x_{i0}$ for various single pass utilizations. It is obvious that the higher the single pass utilization, the higher grows the outlet inert gas concentration $x_i'$ which would allow for a more effective purging of inerts. However, the cell operation becomes unsafe because small changes in $x_{i0}$ may be supposed to occur which would render strong fluctuations of the residual hydrogen

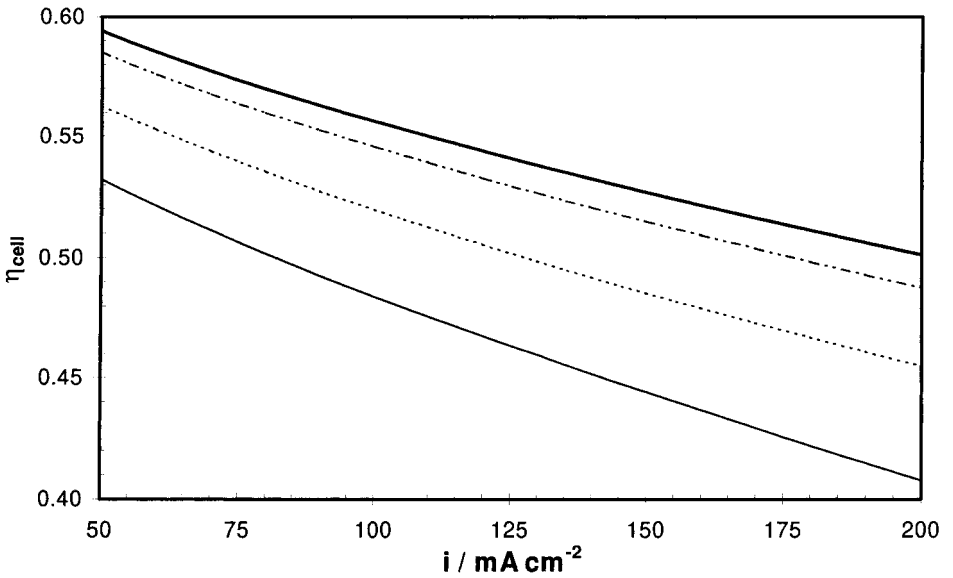


*Fig. 4.* D.c. efficiencies (model) dependent on current density and cell temperature for pure hydrogen, $X_{anode} = 80\%$, $X_{cathode} = 40\%$. Key: (——) 100 °C; (· · · · · ·) 140 °C; (– ·· –) 180 °C; and (——) 200 °C.

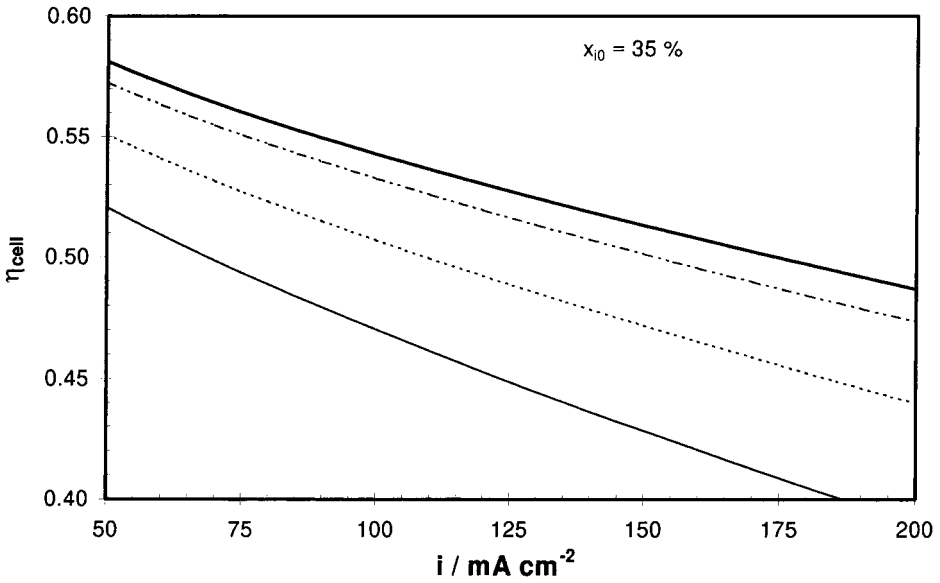


*Fig. 5.* D.c. efficiencies (model) dependent on current density and cell temperature for reformed natural gas, $X_{anode} = 80\%$, $X_{cathode} = 40\%$. Key: (——) 100 °C; (· · · · ·) 140 °C; (– ·· –) 180 °C; and (——) 200 °C.

concentrations at the cell exit at high single pass utilization with the danger of induced high anodic overpotential and corrosion of the cell materials. Therefore, for further consideration, the single pass utilization is set to 80%. Under these conditions, the inert gas fraction of the cycle gas will range from 6 to 60% depending on $x_{i0}$. At 80% single pass utilization the total efficiency $\eta_{d.c.}$ can be described by

$$\eta_{d.c.} = 5 \times 10^{-2} x_{i0} - 1.1 \times 10^{-1} x_{i0}^{0.5} + 0.4615 \qquad (25)$$

According to Equation 25 for $x_{i0} \leq 0.05$, the efficiency loss is almost proportional to the square root of inlet inert gas concentration $x_{i0}$.

3.5.2. *Purge rate effects*

At a given inert gas concentration of the feed, the d.c. efficiency depends on the purge rate. This is depicted in Figures 7 and 8. Figure 7 shows the dependence on the purge rate $\alpha$ for different inert inlet concentrations $x_{i0}$. If the inert gas concentration is low, the hydrogen losses due to purging influences most strongly the cell efficiency. Therefore, at $\alpha = 0.01$ the d.c. efficiency increases by 1% if $x_{i0}$ decreases from 3 to 0.01%. If the cell is operated at $\alpha = 0.05$, the efficiency for $x_{i0} = 3\%$ is by more than half a percent lower than for $\alpha = 0.01$. For $x_{i0} = 0.01$ the efficiency loss for $\alpha = 0.05$ due to purge induced hydrogen ejection is about 1.5% compared to the value at $\alpha = 0.01$.

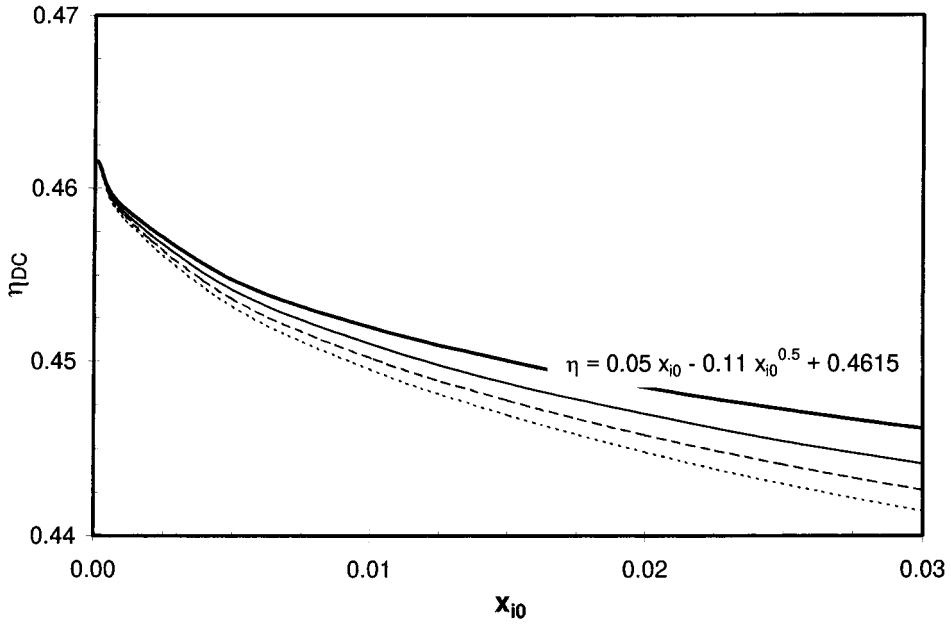


*Fig. 6.* $\eta_{d.c.}$ dependence on hydrogen inlet concentration $x_{i0}$ at optimized purge rates for different single pass utilizations, equation valid for 80% single pass utilization. Key: (——) 90%; (——) 80%; (– – –) 70%; and (· · · · · ·) 60%.

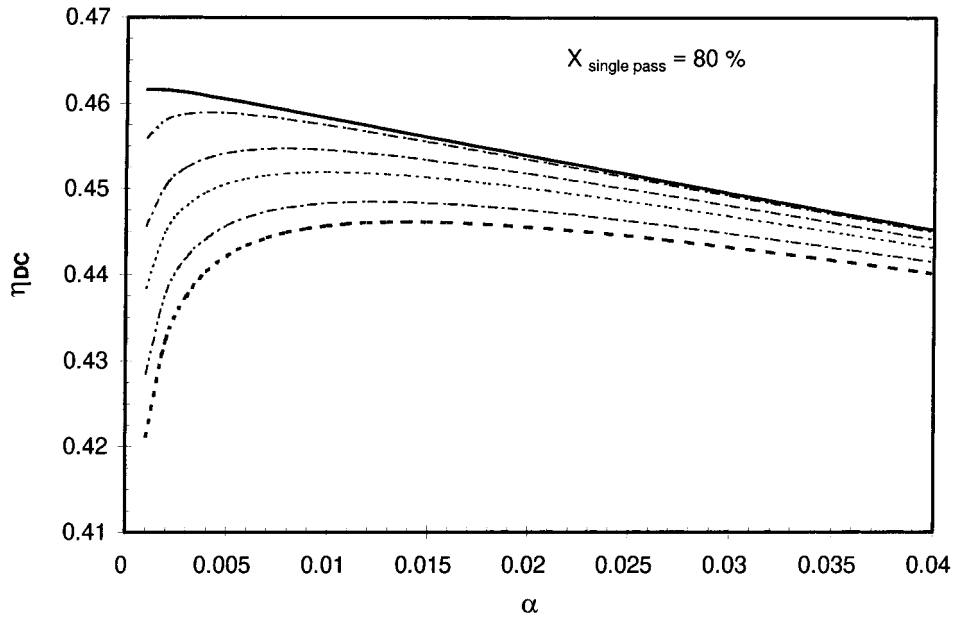


*Fig. 7.* D.c. efficiency dependent on the purge rate $\alpha$ for different $x_{i0}$, at single pass utilization $X_{anode} = 0.8$. Key: (----) 3%; (−··−··) 2%; (·····) 1%; (−·−·−) 0.5%; (−··−··) 0.1%; and (——) 0.01%.

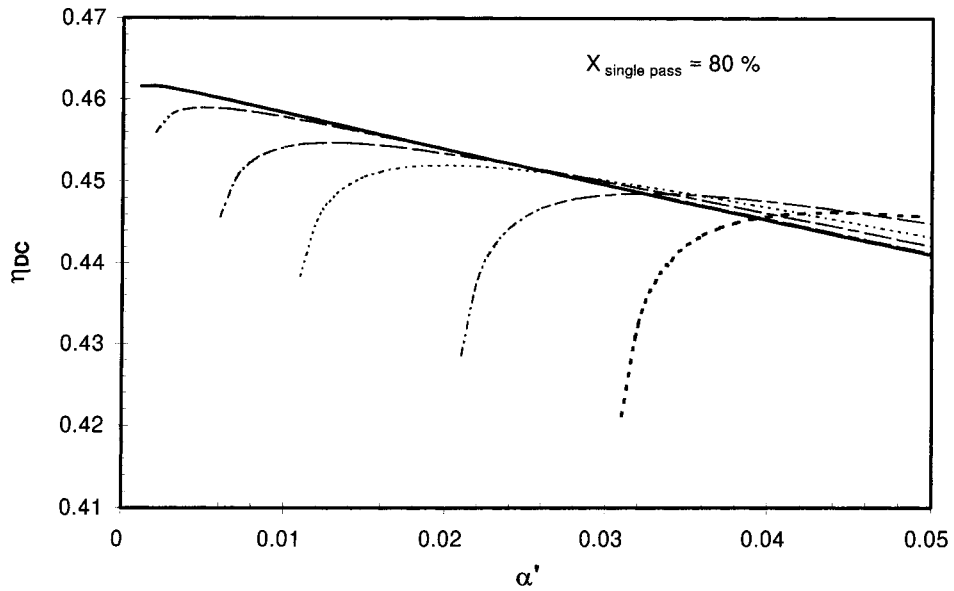


*Fig. 8.* D.c. efficiency dependent on the bleedstream rate $\alpha'$ for different $x_{i0}$ at single pass utilization $X_{anode} = 0.8$. Key: (----) 3%; (−−−−) 2%; (·····) 1%; (−·−·−) 0.5%; (−··−··) 0.1%; and (——) 0.01%.

Now, $\alpha$ in contrast to $\alpha'$ cannot be directly controlled in a technical system. Therefore, Figure 8 recalculates the d.c. efficiency dependency on $\alpha'$ for different inert gas concentrations. It becomes obvious that too low values of $\alpha'$ impair even more severely the d.c. efficiency and also via $x_i'$ the system stability than higher purge rates. Figure 9 shows the optimal bleedstream rate $\alpha'_{opt}$ with $x_{i0}$ for different single pass utilizations. It can be fitted for 80% single pass utilization by

$$\alpha' = 0.8\,x_{i0} + 0.135\,x_{i0}^{0.5} \tag{26}$$

## 4. Conclusion

Summarizing these results, electrical power generation and heat cogeneration by hydrogen fired PAFCs can be realized with electrical cell efficiencies of more than 51% with pure hydrogen at 200 °C and 200 mA cm$^{-2}$ or 100 mW cm$^{-2}$, respectively. Recirculation is possible for hydrogen with only relatively low efficiency losses if hydrogen contains a significant amount of inert gases. High single pass utilization (~80%) is of advantage because of enhanced inert concentrations at the anode outlet. The optimized purge rate increases roughly with the square root of inert gas concentra-

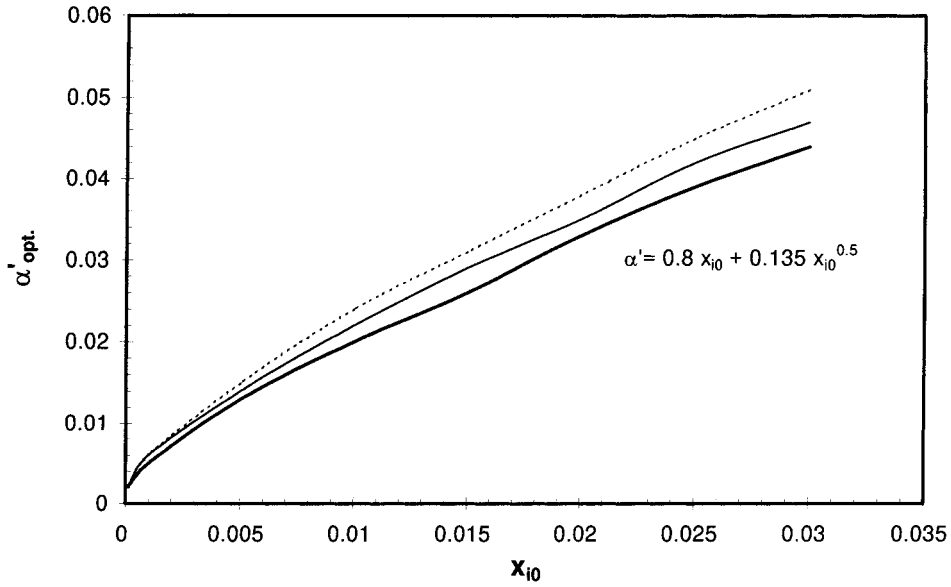


*Fig. 9.* $\alpha'_{opt}$ dependent on $x_{i0}$ for different single pass utilizations, equation valid for 80% single pass utilization. Key: (——) 90%; (——) 80%; and (·····) 60%.

tion. Moreover, decreasing the purge rate $\alpha'$ below the optimal value is more detrimental to the overall electrical efficiency and stable cell operation than enhancing it above $\alpha'_{opt}$. Total efficiency losses increase roughly with the square root of inert gas concentration. The optimal recirculation and bleedstream rates determined in this paper in Figures 7 and 8 would have to be slightly modified in accounting not for cell efficiencies but for whole system efficiencies which would have to include the power consumption of the recirculating blowers.

## Acknowledgement

We gratefully acknowledge the financial support of the Stiftung Energieforschung Baden-Württemberg (Germany).

## References

1. F.A. Brammer, M. Kah and H. Wendt, *Chem. Ing. Tech.* **69** (1997) 1457–62.
2. F.A. Brammer, P. Biehle and M. Steiner, *VDI-Ber (Germany)* **1383** (1988) 83–105.
3. K. Kordesch and S. Simader, *Fuel cells and their applications*, VCH-Verlag, Weinheim, 1996.
4. O. Weinmann and G. Newi, *VDI-Ber (Germany)* **1383** (1998) 129–44.
5. J. Scholta, Dissertation, TH Darmstadt, Darmstadt (1993).
6. J. Scholta and B. Rohland, *in* Proc. 7th Canadian Hydrogen Workshop, 4–6 June 1995, edited by S.K. Metha, T.K. Bose, Canadian Hydrogen Association, Toronto, Canada (1998), pp. 161–9.
7. W. Vogel, J. Lundquist, P. Ross and P. Stonehart, *Electrochim. Acta* **20** (1975) 79–93.